Title

Cellular circadian oscillators in the suprachiasmatic nucleus remain coupled in the absence of connexin-36

Authors

Diemer, Tanja
Landgraf, Dominic
Noguchi, Takako
et al.

Publication Date

2017-08-01

DOI

10.1016/j.neuroscience.2017.05.037

Peer reviewed

Cellular Circadian Oscillators in the Suprachiasmatic Nucleus Remain Coupled in the Absence of Connexin-36

Tanja Diemer[1,#], Dominic Landgraf[1,2,#,*], Takako Noguchi[1], Haiyun Pan[1], Jose L. Moreno[1], and David K. Welsh[1,2]

[1] Department of Psychiatry and Center for Circadian Biology, University of California, San Diego, La Jolla, California, United States of America

[2] Veterans Affairs San Diego Healthcare System, San Diego, California, United States of America,

[#] These authors contributed equally to this work.

* Corresponding author: dolandgraf@gmail.com

Abbreviations:

Cx36 - connexin-36

DD - constant darkness

EM - Explant Medium

GABA - γ-Aminobutyric acid

LD - LD12:12 light/dark cycle (12 hrs light, 12 hrs dark)

LL - constant light

mPer2^{Luc} - PERIOD2::LUCIFERASE

Per2 - Period 2

SCN - Suprachiasmatic nucleus

TTL - transcriptional-translational feedback loop

VIP - vasoactive intestinal peptide

Abstract:

In mammals, the master circadian clock resides in the suprachiasmatic nucleus (SCN). The SCN is characterized by robust circadian oscillations of clock gene expression and neuronal firing. The synchronization of circadian oscillations among individual cells in the SCN is attributed to intercellular coupling. Previous studies have shown that gap junctions, specifically those composed of connexin-36 (Cx36) subunits, are required for short-term coupling of electrical firing among SCN neurons at a time scale of msec. However, it remains unknown whether Cx36 gap junctions also contribute to coupling of longer-term circadian (~24 h) rhythms of clock gene expression. Here, we investigated circadian expression patterns of the clock gene *Period 2* (*Per2*) in the SCN of Cx36-deficient mice using luminometry and single-cell bioluminescence imaging. Surprisingly, we found that synchronization of circadian PER2 expression rhythms is maintained in SCN explants from Cx36-deficient mice. Since Cx36 expression levels change with age, we also tested circadian running-wheel behavior of juvenile and adult Cx36-deficient mice. We found that impact of connexin-36 expression on circadian behavior changes greatly during postnatal development. However, consistent with the intact synchrony among SCN cells in cultured explants, Cx36-deficient mice had intact locomotor circadian rhythms, although adults displayed a lengthened period in constant darkness. Our data indicate that even though Cx36 may be required for electrical coupling of SCN cells, it does not affect coupling of molecular clock gene rhythms. Thus, short-term electrical coupling of neurons and long-term coupling of circadian clock gene oscillations can be regulated independently in the SCN.

Keywords: Circadian, SCN, Coupling, Gap Junctions, Connexin-36

Introduction:

The hypothalamic suprachiasmatic nucleus (SCN) constitutes the central pacemaker of the hierarchically organized mammalian circadian timing system. This system synchronizes circadian rhythms of virtually all neuronal, physiological, humoral, and metabolic processes in the body with each other and with naturally occurring daily rhythms in our environment (Albrecht, 2012). Cellular circadian rhythms in the SCN and all other tissues are based on a core transcriptional–translational feedback loop (TTL) of so called clock genes (Koike, et al., 2012). BMAL1 and CLOCK activate the transcription of *Per1-3* and *Cry1-2*. PER and CRY proteins inhibit BMAL1/CLOCK, and thus their own transcription. Whereas dispersed SCN neurons express circadian rhythms with widely varying periods and phases (Herzog, et al., 1998, Welsh, et al., 1995), neurons in SCN explants are well synchronized and form a coherent oscillator network. Synchronization among SCN neurons depends on strong intercellular coupling (Aton, et al., 2005), which confers resistance to genetic and environmental perturbations (Aton and Herzog, 2005, Liu, et al., 2007). Various mechanisms for the intercellular coupling of SCN neurons have been suggested, including neuronal firing and synaptic release of the neurotransmitter γ-Aminobutyric acid (GABA) and various neuropeptides, especially vasoactive intestinal peptide (VIP). However, circadian clocks in the developing SCN are fully functional and apparently synchronized long before neurochemical synaptic connections are present (Landgraf, et al., 2015, Landgraf, et al., 2014, Moore and Bernstein, 1989), suggesting the existence of an additional mechanism for cell communication within the SCN. Several studies implicate gap junctions in such a role.

Gap junctions are protein complexes functioning as pores to connect the cytoplasm of two cells and allow passage of ions and small molecules between them. These so called electrical synapses are composed of connexin subunits and are found throughout the brain and the rest of the body. The SCN expresses a number of different connexins (Colwell, 2000, Rash, et al., 2007, Welsh and Reppert, 1996). Although SCN neurons are not coupled by gap junction channels in dissociated cultures (Welsh and Reppert, 1996), gap junction coupling in intact SCN tissue has been demonstrated with tracer molecules and by electrical stimulation and recording

of neighboring cells (Colwell, 2000, Jiang, et al., 1997, Shinohara, et al., 2000). Furthermore, electrical coupling between neurons of cultured SCN explants can be suppressed with carbenoxolone, a reversible blocker of gap junctions (Wang, et al., 2014). In particular, connexin-36 (Cx36) has been reported to play a crucial role in electrical coupling of SCN neurons. Knockout of Cx36 blocks intercellular electrical coupling between SCN neurons, and adult *Cx36*$^{-/-}$ mice display a lower amplitude of circadian locomotor activity rhythms and a decrease of overall activity under constant environmental conditions (Long, et al., 2005). Based on these studies, it was hypothesized that due to coordinated firing of SCN neurons, gap junctions, in particular those composed of Cx36, contribute to the regulation of behavioral, hormonal, and autonomic circadian rhythms (Colwell, 2000, Jiang, et al., 1997, Long, et al., 2005). On the other hand, in the rodent hypothalamus, Cx36 is mainly expressed during early development (Belluardo, et al., 2000), and the SCN of adult mice shows only weak dye coupling and very small gap junctions (Rash, et al., 2007). Furthermore, although Cx36 was shown to be crucial for electrical coupling, it has not been demonstrated directly whether it also contributes to synchronization of molecular clock gene rhythms between individual SCN neurons.

In this study, we further investigated the role of Cx36 within the SCN and tested directly whether it is involved in synchronization of clock gene rhythms between cells. To do this, we measured the expression of the clock gene *Per2* in individual cells of SCN explants cultured from newborn *Cx36*$^{-/-}$ mice carrying a PERIOD2::LUCIFERASE (*mPer2*^{Luc}) reporter gene. We also measured *mPer2*^{Luc} patterns of entire SCN explants from newborn mice. Since gap junctions may be primarily important for SCN cell coupling at early developmental stages, we compared behavioral rhythms of juvenile and adult *Cx36*$^{-/-}$ mice under different environmental lighting conditions. In contrast to the established role of Cx36 in short-term synchronization of action potentials of SCN neurons, our data suggest that Cx36 is not required for more long-term synchronization of circadian clock gene rhythms in SCN cells. This result is supported by the finding that knockout of Cx36 has only relatively mild effects on behavioral rhythms, even in juvenile mice when Cx36 expression is presumably higher than in adults.

Experimental procedures:

Animals:

For bioluminescence experiments, *Cx36*$^{-/-}$ mice (Deans, et al., 2001) were crossed to mPer2^{Luc} -SV40 reporter mice (Welsh, et al., 2004, Yoo, et al., 2004). The mice were backcrossed >10 generations to the B6 strain. Throughout the text, for convenience, these mice will be referred to as wild-type, *Cx36*$^{+/-}$, and *Cx36*$^{-/-}$ mice. Running-wheel experiments were conducted with mice not carrying the mPer2^{Luc} reporter. All mice used in this study were male and female wild-type, *Cx36*$^{+/-}$, and *Cx36*$^{-/-}$ littermates. SCN cultures for *mPer2*^{Luc} bioluminescence measurements and imaging were from neonatal (3-6 day old) male and female mice. In the behavioral assay, male and female mice were used, juvenile mice were 3-4 weeks old, and adult mice were 9-30 weeks old at the beginning of the experiment. If not otherwise stated, mice were maintained in LD 12:12 cycles (12 h light, 12 h dark). Food and water was available *ad libitum*. Mouse studies were approved by the Institutional Animal Care and Use Committee at University of California, San Diego (Protocol number: S07365). Every effort was made to minimize the number of animals used, and their suffering.

SCN culture:

Brains were removed, blocks of ventral hypothalamus were prepared, and 250 µm brain slices were cut with razor blades mounted on a tissue chopper (Stoelting, Wood Dale, IL, USA). Sections containing SCN tissue were trimmed with a curved scalpel blade to ~2 mm x 2 mm. Each slice was then placed gently on a tissue culture insert (EMD Millipore, Billerica, MA, USA) in a 35 mm culture dish containing ~1 ml Explant Medium (EM) formulated for equilibration with air (high glucose DMEM [Mediatech, Manassas, VA, USA], 4 mM sodium carbonate, 10 mM HEPES, 52 U/ml penicillin, 52 µg/ml streptomycin, 4 mM L-glutamine, 2% B-27 [GIBCO, Grand Island, NY, USA], 0.1 mM luciferin [BioSynth, Itasca, IL, USA]) and cultured at 37˚C, 0% CO_2.

mPer2^{Luc} *bioluminescence imaging:*

Single-cell mPer2^{Luc} measurements were carried out as described elsewhere (Noguchi, et al., 2013, Welsh and Noguchi, 2012) with a few modifications. Light from the sample was collected

by an Olympus UPlanSApo 10x objective (NA 0.40). Images were collected at intervals of 30 min, with 29.5 min exposure duration, for 6-15 days without binning (binning 1x1). Images were analyzed with MetaMorph (Molecular Devices, Sunnyvale, CA, USA) as described previously (Evans, et al., 2012). Period, phase, goodness of fit, and amplitude were determined over 5 days by fitting a sine wave [Sin fit (Damped) for period, phase, and goodness of fit, or LM fit (Sin) for amplitude] to 24 h running average baseline-subtracted data using LumiCycle Analysis software (Actimetrics, Wilmette, IL, USA). The first day of measurement was excluded from analyses.

mPer2^{Luc} measurements in LumiCycle luminometer:

Luminescence measurements were taken over 10 min intervals using a LumiCycle luminometer (Actimetrics) that was placed inside an incubator kept at 36°C. Period, peak phases, goodness of fit, and amplitude were determined over 5 days as described above. Amplitude was normalized to total brightness in order to account for different sizes of brain tissue and technical differences between slices. Sin fit (Damped) sine wave fit was used to calculate the damping constant (time to reach 1/e of initial amplitude).

Behavioral assay:

Mice were singly housed in running wheel-equipped cages, and locomotor activity was monitored under various lighting conditions. First, juvenile (3-4 weeks old at beginning of experiment) and adult mice (9-30 weeks old) were kept under LD 12:12 conditions for 14 days. Light levels were 800 lux. Mice were then kept in constant darkness (DD) for at least 20 days. During DD experiments, daily health checks of mice were done at irregular times and under dim red light. After DD, adult mice (22-28 weeks old) were kept again in LD for 21 days and then transferred to constant light conditions (LL). In LL, Light levels were gradually increased from 200 lux to 400 lux to 600 lux every 14 days. Wheel-running activity was analyzed using ClockLab software (Actimetrics, USA). Period was calculated based on the χ^2 periodogram method. Amplitude was calculated as described previously (Long, et al., 2005). The phase angle of entrainment in LD was calculated by fitting a regression line to the activity onsets. Total activity is presented as total wheel revolutions per day. The first 4 days of the experiments were

excluded from analysis. The number of analyzed days is indicated in the figure legends. The same days were analyzed for each animal.

Data analysis:

Statistical analysis was carried out with GraphPad Prism (GraphPad Software, USA) and Oriana (KCS, Pentraeth, UK). Statistical tests, F-values, degrees of freedom, n-values and p-values for each experiment are indicated in the figure legends.

Results:

Connexin-36 is not required for intercellular coupling of SCN molecular circadian oscillators

In the SCN oscillator network, circadian rhythms of neuronal activity and expression of clock genes are synchronized among cells (Aton and Herzog, 2005). Precise, short-term intercellular synchronization of neuronal activity requires Cx36, and electrical coupling between SCN neurons is interrupted in *Cx36*$^{-/-}$ mice (Long, et al., 2005). To investigate whether Cx36 is also involved in long-term synchronization of circadian clock gene expression rhythms in the SCN, we crossed *Cx36*$^{-/-}$ mice with the mPer2^{Luc} reporter line and obtained *Cx36*$^{-/-}$ mice bearing the bioluminescent PER2 reporter. We measured mPer2^{Luc} rhythms in individual cells of organotypic SCN explants from neonatal wild-type, *Cx36*$^{+/-}$, and *Cx36*$^{-/-}$ mice. Single cells from *Cx36*$^{+/-}$ and *Cx36*$^{-/-}$ mice displayed significantly longer periods than cells from wild-type mice, but variability of periods across cells was comparably low in all three genotypes, suggesting intact intercellular coupling. Amplitude and goodness of fit were unaffected in *Cx36*$^{+/-}$ and *Cx36*$^{-/-}$ mice (Fig. 1A). As another measure of intercellular coupling of molecular clocks, we quantified the phase clustering of cellular mPer2^{Luc} peaks on day 5 of culture on the basis of the length of the mean vector of a Rayleigh Plot. Interestingly, phase clustering of single SCN cells from *Cx36*$^{+/-}$and *Cx36*$^{-/-}$ mice was not different from that of cells from wild-type mice, suggesting equally strong coupling of molecular oscillators among cells in all three genotypes (Fig. 1B, C, *supplemental videos*). Notably, synchronization among cells remained similarly stable over at least 15 days in wild-type, *Cx36*$^{+/-}$, and *Cx36*$^{-/-}$ mice, further demonstrating robust coupling within the molecular oscillator network in all three genotypes over time (Fig. 1D, *supplemental videos*).

Overall Per2 output of the SCN clock network is unaffected by reduced expression of Cx36

To determine whether the total output of the molecular SCN clock network is influenced by reduction or absence of Cx36, we monitored the total mPer2^{Luc} bioluminescence pattern of entire organotypic SCN explants from neonatal wild-type, *Cx36*$^{+/-}$, and *Cx36*$^{-/-}$ mice. Reduced synchronization among single cells would be reflected in lower amplitude, lower goodness of

fit, and faster damping (shorter damping constant) of the mPer2^{Luc} signal from an SCN explant cell population. However, period, amplitude, goodness of fit, and damping were unaffected in *Cx36*$^{+/-}$ and *Cx36*$^{-/-}$ mice, relative to wild type mice (Fig. 2). In fact, many samples of all three genotypes increased amplitude over time, leading to negative damping constants. For this reason, the average damping constant of each genotype is close to 0, indicating no net damping on average. These findings further indicate that Cx36 does not contribute to coupling or synchronization of circadian rhythms of clock gene expression in SCN cells.

Contrasting effects of loss of Cx36 on circadian behavior in juvenile and adult mice

Previous work by Long et al. (2005) demonstrated that loss of Cx36 affects circadian running wheel behavior in mice. In that study, *Cx36*$^{-/-}$ mice displayed a slight, but significant, lengthening of period under LD conditions and a significant reduction of free-running amplitude in DD. In addition, *Cx36*$^{-/-}$ mice exhibited decreasing levels of activity with time in DD (Long, et al., 2005). However, *Cx36* expression in the brain decreases during development (Belluardo, et al., 2000), and we therefore expected that effects of SCN gap junctions on circadian behavior might vary with age. Accordingly, we examined circadian rhythms of running wheel behavior in both juvenile and adult mice under similar experimental conditions in our laboratory. In juvenile mice, we found that behavioral circadian period was similar across wild-type, *Cx36*$^{+/-}$, and *Cx36*$^{-/-}$ genotypes (Fig. 3A, B). Initially (in LD), behavioral rhythm amplitude of juvenile *Cx36*$^{-/-}$ mice was significantly decreased relative to wild-type mice, but then both circadian amplitude and amount of behavioral activity of juvenile *Cx36*$^{-/-}$ mice increased over time in DD, such that by days 11-20 of DD, both were significantly higher than in wild-type controls (Fig. 3A, B). In addition, the onset of activity in LD was significantly later in *Cx36*$^{+/-}$ mice compared to wild-type and *Cx36*$^{-/-}$ mice (Fig. 3C). In contrast, compared to adult wild-type mice, adult *Cx36*$^{-/-}$ mice showed significantly longer free-running periods in DD, reduced total activity in LD and DD, but no significant changes in amplitude under any lighting conditions (Fig. 3D, E). Activity onset in LD was not differently timed across genotypes in adult mice (Fig. 3F). These contrasting behavioral phenotypes of juvenile and adult *Cx36*$^{-/-}$ mice suggest a complex developmental change in how neuronal gap junctions influence circadian rhythms of locomotor activity.

Stability of behavioral rhythms is not impaired by loss of Connexin-36

So far, our results from cultured SCN explants and behavioral rhythms in DD do not suggest that suppression of Cx36 affects coupling of molecular oscillators among SCN neurons or the robustness of rest/activity rhythms. Since constant culture conditions and DD may not be challenging enough to provoke uncoupling of *Cx36*$^{-/-}$ SCN cells, we exposed *Cx36*$^{-/-}$ mice to constant illumination and measured their circadian behavior rhythms. Constant light is able to disturb synchronization of SCN neurons and can (dependent on light intensity) thereby cause low amplitude or total loss of circadian behavioral rhythms in mammals (Albers, et al., 1981, Ohta, et al., 2005, Rosenwasser, 1993, Sudo, et al., 2003). Thus, if *Cx36*$^{-/-}$ mice have neuronal coupling deficits in the SCN, they should react more sensitively to constant light than wild-type mice and show much lower rhythm amplitudes. For our experiment, we used constant light with increasing intensities (200 lux, 400 lux, 600 lux, 14 days each). Interestingly, period, amplitude, and total activity levels were not significantly different in wild-type and *Cx36*$^{-/-}$ mice at any light intensity (Fig. 4A, B). This result suggests that rhythms of the SCN oscillator network of both genotypes are equally stable even under challenging LL conditions.

Discussion:

Coupling of cellular circadian clocks within the SCN neuronal network is the basis of the SCN's uniquely robust circadian oscillations (Buhr, et al., 2010, Liu, et al., 2007). Previous work has suggested various possible coupling mechanisms, including gap junctions: intercellular channels composed of connexins that permit free passage of ions and small molecules between cells. Long et al. (2005) demonstrated that Cx36 gap junctions are critically involved in short-term synchronization of electrical activity between SCN cells. A particularly important role has been assigned to Cx36, as SCN neurons of *Cx36*$^{-/-}$ mice fail to transmit electrical impulses from one cell to another (Long, et al., 2005). Here, however, we provide evidence that, in contrast to short-term synchronization of neuronal firing, long-term synchronization of circadian clock gene expression rhythms among cells in the SCN is unaffected by the absence of Cx36.

Our experiments indicate that mPer2^{Luc} oscillations of individual cells in SCN explants are equally well coupled in wild-type, *Cx36*$^{+/-}$ and *Cx36*$^{-/-}$ mice. While the circadian periods of individually measured SCN cells of *Cx36*$^{+/-}$ and *Cx36*$^{-/-}$ mice are overall longer than in wild-type SCN explants, rhythms of all cells are synchronized with one another over the course of many days. This result is confirmed by measurements of the total mPer2^{Luc} output of SCN explants, which showed no indications of desynchronization among individual oscillators.

Furthermore, circadian locomotor activity behavior of *Cx36*$^{+/-}$ and *Cx36*$^{-/-}$ mice shows little evidence for impairment of coupling between cells of the SCN oscillator network. Cx36 expression is higher in the brains of young rodents (Belluardo, et al., 2000). *Cx36*$^{-/-}$ mice tested soon after weaning, the earliest age at which they are able to run on wheels, do show modestly reduced behavioral rhythm amplitude in LD. However, only a few weeks later, *Cx36*$^{-/-}$ mice actually show higher circadian rhythm amplitude in DD. Even in LL, a condition that provokes desynchronization of SCN neurons (Ohta, et al., 2005), wild-type, *Cx36*$^{+/-}$ and *Cx36*$^{-/-}$ mice exhibited no differences in their circadian behavior. These data show that, at least in adult mice, Cx36 is not required for coupling of molecular rhythms in SCN neurons. Although our behavioral data cannot exclude the possibility that Cx36 gap junctions may play a role in

coupling of SCN cellular oscillators in very young mice, more direct measurements of coupling in SCN explants fail to show any evidence for such a role.

Moreover, because the loss of Cx36 affects all brain regions and all other tissues of these animals, effects on amplitude of behavioral rhythms in *Cx36*$^{-/-}$ mice are difficult to interpret, and may not necessarily be related to intrinsic SCN function. Juvenile *Cx36*$^{-/-}$ mice display increased overall levels of activity in DD, which may contribute to increased amplitude of their rest/activity cycles. Possibly, these mice are overactive due to impairments in other brain areas, but the SCN clock is still strong enough to suppress activity during the subjective sleep time, leading to a pronounced difference in activity levels between subjective day and night time. In adult *Cx36*$^{-/-}$ mice, total activity is significantly reduced, and these mice show either no amplitude effects (our study) or a decrease of amplitude (Long, et al., 2005). Just as for the increased amplitude we observed in juvenile *Cx36*$^{-/-}$ mice in DD, reduced amplitude in juvenile *Cx36*$^{-/-}$ mice in LD conditions (our study) or in adult *Cx36*$^{-/-}$ mice (Long, et al., 2005) may be related to deficiencies outside the SCN, e.g. in the light input pathway in the retina (O'Brien, 2014), and not necessarily due to altered coupling among SCN cells.

Even though changes in amplitude of behavioral rhythms cannot necessarily be attributed to the SCN, it is remarkable that the behavioral phenotypes of juvenile and adult mice are so different. Whereas juvenile *Cx36*$^{-/-}$ mice display increased activity levels and higher amplitude in DD, adult mice show decreased activity levels and a tendency to lower amplitude in our study. The amplitude decrease in adult *Cx36*$^{-/-}$ mice in DD was significant in the study of Long et al., 2005. In addition, a reduction of Cx36 in *Cx36*$^{+/-}$ mice seems to have a stronger impact on the onset of activity in LD in juvenile mice than in adult mice. Possibly related to altered expression levels of Cx36 throughout postnatal development (Belluardo, et al., 2000), the behavioral effects of Cx36 seem to change drastically.

In our study, we also find different period effects than described in Long et al. (Long, et al., 2005). We find a lengthened circadian period in locomotor activity compared to controls in DD,

which was not reported previously. Such different results may occur due to technical differences between the two studies. Long et al. used mice with a mixed B6/129 background, whereas our mice were backcrossed >10 generations to B6. Furthermore, Long et al. did not specify gender, whereas we used males and females. Importantly, similar to our results, Long et al. did report a lengthening of the circadian period of *Cx36*$^{-/-}$ mice in the first 10 days after the transition to DD in one of their animal cohorts. A summary of our results and the results of Long et al., 2005 is shown in Fig. 5.

Taken together, our results and the results of previous studies suggest the existence of different coupling mechanisms responsible for electrical coupling and for coupling of molecular clock gene rhythms. Whereas it was convincingly shown that Cx36 gap junctions contribute to electrical coupling (Long, et al., 2005, Wang, et al., 2014), our data suggest that they are not involved in synchronization of clock gene rhythms. Other factors that are involved in neuronal coupling in the SCN are the neurotransmitters GABA and VIP, which are both strongly expressed by most SCN neurons. GABA contributes to the synchronization of electrical activity of SCN neurons in the dorsal and the ventral regions of the SCN (Albus, et al., 2005), and SCN cells excited by GABA form clusters that retain synchrony over time (DeWoskin, et al., 2015). Genetic elimination of VIP signaling leads to desynchronization of circadian rhythms among SCN neurons (Aton, et al., 2005, Brown, et al., 2007, Pauls, et al., 2014), and reconstitution of VIP signaling in VIP-deficient SCN grafts restores rhythmicity and synchronization of molecular PER2 rhythms (Maywood, et al., 2011).

Of note, SCN neuron electrical activity and clock gene expression influence each other mutually. For example, the elimination of the clock gene *Per1* disrupts the synchronization of molecular and electrical circadian rhythms in SCN neurons (Jones and McMahon, 2016). Manipulating the firing rate of SCN neurons alters circadian rhythms of clock gene expression and rest/activity behavior (Jones, et al., 2015). Because of such mutual interactions, assigning putative coupling factors strictly to either electrical or molecular coupling is not possible. Rather, gap junctions, neurotransmitters like GABA and VIP, and other factors likely form a complex system that

facilitates both electrical and molecular coupling, thus providing the basis of robust synchronization among cells in the SCN oscillator network.

In summary, our results demonstrate that synchronization of clock gene expression rhythms among SCN cells is not dependent on Cx36. Even in the complete absence of Cx36, mPer2^{Luc} rhythms of individual SCN cells are still well synchronized, and the total mPer2^{Luc} output of SCN explants shows no indication of desynchrony. Instead, as Cx36 was previously shown to be crucial for electrical coupling of SCN neurons, Cx36 seems to be primarily involved in short-term synchronization of firing of SCN neurons (Fig. 6). Thus, in the absence of Cx36 gap junctions, even though short-term firing synchrony among SCN neurons is reduced or absent (Long, et al., 2005), we found that long-term synchrony of clock gene rhythms is preserved. Experimentally, it is difficult to distinguish clearly between electrical and circadian coupling, because of mutual interactions between SCN electrical activity and the molecular circadian clock. However, our data indicate that electrical and circadian coupling can be regulated independently to some extent, such that lack of synchronized electrical activity in the SCN does not necessarily imply lack of synchronized clock gene expression. Further *in vitro* studies with simultaneous long-term recordings of neuronal activity and clock gene rhythms will likely clarify the full subtleties of interplay of electrical and molecular rhythms in the SCN.

Figure captions:

Figure 1: SCN cells show stable coupling of molecular rhythms in *Cx36*$^{+/-}$ and *Cx36*$^{-/-}$ mice. All data presented in this figure are from the same SCN explants. **(A)** Mean circadian period, amplitude, and sine wave goodness-of-fit of cellular mPer2^{Luc} rhythms of cells in SCN explants from wild-type (black), *Cx36*$^{+/-}$ (orange), and *Cx36*$^{-/-}$ (red) mice. Data are shown as mean ± SEM. Period: $F_{2,173}$ = 17.71, p = <0.0001, post hoc: ***p ≤ 0.001. Amplitude: $F_{2,173}$ = 0.2086, p = 0.8119, post hoc: not significant. Goodness of fit: $F_{2,173}$ = 2.947; p = 0.0552, post hoc: not significant. One-way-ANOVA with Bonferroni post hoc test comparing all data sets with each other; wild-type: n = 77/4 (cells/explants); *Cx36*$^{+/-}$: n = 40/2; *Cx36*$^{-/-}$: n = 59/3. **(B)** Mean vector length of phase distribution of cellular mPer2^{Luc} rhythms of cells in SCN explants on day 5 of *in vitro* culture. Data are shown as mean ± SEM. $F_{2,6}$ = 1.177, p = 0.3705, post hoc: not significant. One-way-ANOVA with Bonferroni post hoc test comparing all data sets with each other; wild-type: n = 4; *Cx36*$^{+/-}$: n = 2; *Cx36*$^{-/-}$: n = 3. **(C)** Phase distribution of single cells from different SCN explants. Data are shown as Rayleigh plots with circles representing 24 h of day 5 of *in vitro* culture and each triangle representing the mPer2^{Luc} peak phase (time of day) of an individual cell. Cells from different explants are shown in different colors. Each vector represents the average peak time of cells from an SCN explant, and the vector length represents the phase clustering. A longer vector means greater concentration of the data near the mean, and thus less likelihood of the data being uniformly distributed. **(D)** Raster plots of mPer2^{Luc} bioluminescence intensity of individual wild-type (left, n = 25), *Cx36*$^{+/-}$ (center, n = 20), and *Cx36*$^{-/-}$ (right, n = 20) SCN cells in one slice per genotype. Each horizontal line represents a single cell, with time in days in culture plotted left to right. Values above and below the mean are shown in red and green, respectively.

Figure 2: Total mPer2^{Luc} rhythm of SCN explants is not altered in *Cx36*$^{+/-}$ and *Cx36*$^{-/-}$ mice. Mean circadian period, amplitude, sine wave goodness-of-fit, and the damping constant of mPer2^{Luc} rhythms of SCN explants from wild-type (black), *Cx36*$^{+/-}$ (orange), and *Cx36*$^{-/-}$ (red) mice. Data are shown as mean ± SEM. PERIOD: $F_{2,18}$ = 0.4747, p = 0.6297, post hoc: not significant. AMPLITUDE: $F_{2,18}$ = 0.4256, p = 0.6598, post hoc: not significant. GOODNESS OF FIT: $F_{2,18}$ = 0.2564; p = 0.7766, post hoc: not significant. DAMPING: $F_{2,18}$ = 0.02619; p = 0.9742, post hoc: not significant. One-way-ANOVA with Bonferroni post hoc test comparing all data sets with each other; wild-type: n = 4; *Cx36*$^{+/-}$: n = 10; *Cx36*$^{-/-}$: n = 7.

Figure 3: Loss of Connexin-36 affects circadian behavior of juvenile and adult mice differently. **(A)** Representative double-plotted actograms showing wheel-running activity of juvenile wild-type (left), *Cx36*$^{+/-}$ (center), and *Cx36*$^{-/-}$ (right) mice in a light/dark cycle (LD) and then in constant darkness (DD). Gray areas represent darkness. **(B)** Mean circadian period, amplitude, and total activity levels of circadian behavioral rhythms from juvenile wild-type (black), *Cx36*$^{+/-}$ (orange), and *Cx36*$^{-/-}$ (red) mice in LD and in DD (days 1-10 and days 11-20) (gray areas). Data are shown as mean ± SEM. PERIOD: Interaction: $F_{4,19} = 1.624$, $p = 0.1883$. Light conditions: $F_{2,19} = 46.24$, $p < 0.0001$. Genotype: $F_{2,19} = 0.8834$, $p = 0.4297$; post hoc: not significant. AMPLITUDE: Interaction: $F_{4,19} = 21.37$, $p < 0.0001$; Light conditions: $F_{2,19} = 28.67$, $p < 0.0001$; Genotype: $F_{2,19} = 0.3034$, $p = 0.7411$; post hoc: *p ≤ 0.05, **p ≤ 0.01, ***p ≤ 0.001. ACTIVITY LEVELS: Interaction: $F_{4,19} = 10.52$, $p < 0.0001$; Light conditions: $F_{2,19} = 53.81$, $p < 0.0001$; Genotype: $F_{2,19} = 1.357$, $p = 0.2813$; post hoc: ***p ≤ 0.001 (2-way repeated measurement ANOVA); wild-type: n = 8; *Cx36*$^{+/-}$: n = 6; *Cx36*$^{-/-}$: n = 8. **(C)** Mean phase angle of entrainment in LD of circadian behavioral rhythms from the same animals as in (B). Data are shown as mean ± SEM. $F_{2,19} = 5.825$, $p = 0.0106$, post hoc: *p ≤ 0.05. One-way-ANOVA with Bonferroni post hoc test comparing all data sets with each other. **(D)** Representative double-plotted actograms showing wheel-running activity of adult wild-type (left), *Cx36*$^{+/-}$ (center), and *Cx36*$^{-/-}$ (right) mice in LD and DD. Gray areas represent darkness. **(E)** Mean circadian period, amplitude, and total activity levels of circadian behavioral rhythms from adult wild-type (black), *Cx36*$^{+/-}$ (orange), and *Cx36*$^{-/-}$ (red) mice in LD and in DD (days 1-10 and days 11-20) (gray areas). Data are shown as mean ± SEM. PERIOD: Interaction: $F_{4,29} = 2.560$, $p = 0.0479$; Light conditions: $F_{2,29} = 58.59$, $p < 0.0001$; Genotype: $F_{2,29} = 6.611$, $p = 0.0043$; post hoc: *p ≤ 0.05, **p ≤ 0.01, ***p ≤ 0.001. AMPLITUDE: Interaction: $F_{4,29} = 0.9396$, $p = 0.4476$; Light conditions: $F_{2,29} = 11.30$, $p < 0.0001$; Genotype: $F_{2,29} = 2.580$, $p = 0.0931$; post hoc: not significant. ACTIVITY LEVELS: Interaction: $F_{4,29} = 0.3328$, $p = 0.8548$; Light conditions: $F_{2,29} = 1.077$, $p = 0.3475$; Genotype: $F_{2,29} = 5.951$, $p = 0.0068$; post hoc: *p ≤ 0.05, **p ≤ 0.01 (2-way repeated measurement ANOVA); wild-type: n = 10; *Cx36*$^{+/-}$: n = 10; *Cx36*$^{-/-}$: n = 12. **(F)** Mean phase angle of entrainment in LD of circadian behavioral rhythms from the same animals as in (E). Data are shown as mean ± SEM. $F_{2,29} = 1.094$, $p = 0.3483$, post hoc:

not significant. One-way-ANOVA with Bonferroni post hoc test comparing all data sets with each other.

Figure 4: Robustness of behavioral rhythms is not impaired in *Cx36*$^{-/-}$ mice in constant light. **(A)** Representative double-plotted actograms showing wheel-running activity of wild-type (left), *Cx36*$^{+/-}$ and *Cx36*$^{-/-}$ (right) mice in constant light after prior entrainment in light/dark. Yellow areas represent light. Increasing brightness of yellow areas represents increasing light intensities from 200 lux to 400 lux to 600 lux (14 days each). **(B)** Mean circadian period, amplitude, and total activity levels of circadian behavioral rhythms from wild-type (black) and *Cx36*$^{-/-}$ (red) mice in LD and in LL (yellow areas). Data are shown as mean ± SEM. PERIOD: Interaction: $F_{3,11} = 0.1389$, $p = 0.9360$; Light conditions: $F_{3,11} = 2.119$, $p = 0.1167$; Genotype: $F_{1,11} = 0.4167$, $p = 0.5318$; post hoc: not significant. AMPLITUDE: Interaction: $F_{3,12} = 0.3861$, $p = 0.7636$; Light conditions: $F_{3,12} = 32.51$, $p < 0.0001$; Genotype: $F_{1,12} = 0.8797$, $p = 0.3668$; post hoc: not significant. ACTIVITY LEVELS: Interaction: $F_{3,12} = 0.08383$, $p = 0.9684$; Light conditions: $F_{3,12} = 48.27$, $p < 0.0001$; Genotype: $F_{1,12} = 1.366$, $p = 0.2652$; post hoc: not significant (2-way repeated measurement ANOVA); wild-type: n = 7/8; *Cx36*$^{-/-}$: n = 6.

Figure 5: Comparison of results from mPer2^{Luc} measurements of single SCN cells and whole SCN explants with behavioral phenotypes from juvenile (3-4 weeks old at the beginning of the experiment) and adult mice from this study (9-30 weeks old) and adult mice from Long et al., 2005 (19-25 weeks old).

Figure 6: Simplified scheme of mechanisms that control electrical and molecular coupling of SCN neurons. Two adjacent SCN neurons with clock genes that comprise a transcriptional-translational feedback loop (TTL). Propagating action potentials are presented as yellow lightning bolts. Pink insets: circadian mPer2^{Luc} rhythms from cell 1 and cell 2. Yellow insets: short-term patterns of action potentials from cell 1 and cell 2, as shown in Long et al., 2005 and Wang et al., 2014. **(A)** In the presence of Cx36 gap junctions, electrical activity and clock gene rhythms of SCN neurons are both coupled between cells. Molecular rhythms of clock genes are presumably mainly synchronized by neurotransmitters like GABA and VIP. **(B)** In the absence of functional gap junctions, clock gene rhythms are still synchronized by GABA and VIP. However, electrical activity is no longer synchronized, and cells fire with different patterns.

Acknowledgement:

Funding: This study was supported by NIH (R01 MH082945 to DKW), a V.A. Career Development Award (DKW), and a NARSAD Young Investigator Award (DKW). The funders had no role in study design, data collection and analysis, decision to publish, or preparation of the manuscript.

Author contribution: Conceived and designed the experiments: DKW, TD. Performed the experiments: TD, DL, TN, HP, JLM. Analyzed the data: DL. Wrote the paper: DL, DKW. We thank Elizabeth M. Harrison for help with analysis of behavioral data.

References:

H.E. Albers, A.A. Gerall, J.F. Axelson, Circadian rhythm dissociation in the rat: effects of long-term constant illumination, Neuroscience letters, 25 (1981) 89-94.

U. Albrecht, Timing to perfection: the biology of central and peripheral circadian clocks, Neuron, 74 (2012) 246-260.

H. Albus, M.J. Vansteensel, S. Michel, G.D. Block, J.H. Meijer, A GABAergic mechanism is necessary for coupling dissociable ventral and dorsal regional oscillators within the circadian clock, Current biology : CB, 15 (2005) 886-893.

S.J. Aton, C.S. Colwell, A.J. Harmar, J. Waschek, E.D. Herzog, Vasoactive intestinal polypeptide mediates circadian rhythmicity and synchrony in mammalian clock neurons, Nature neuroscience, 8 (2005) 476-483.

S.J. Aton, E.D. Herzog, Come together, right...now: synchronization of rhythms in a mammalian circadian clock, Neuron, 48 (2005) 531-534.

N. Belluardo, G. Mudo, A. Trovato-Salinaro, S. Le Gurun, A. Charollais, V. Serre-Beinier, G. Amato, J.A. Haefliger, P. Meda, D.F. Condorelli, Expression of connexin36 in the adult and developing rat brain, Brain research, 865 (2000) 121-138.

T.M. Brown, C.S. Colwell, J.A. Waschek, H.D. Piggins, Disrupted neuronal activity rhythms in the suprachiasmatic nuclei of vasoactive intestinal polypeptide-deficient mice, Journal of neurophysiology, 97 (2007) 2553-2558.

E.D. Buhr, S.H. Yoo, J.S. Takahashi, Temperature as a universal resetting cue for mammalian circadian oscillators, Science, 330 (2010) 379-385.

C.S. Colwell, Rhythmic coupling among cells in the suprachiasmatic nucleus, Journal of neurobiology, 43 (2000) 379-388.

M.R. Deans, J.R. Gibson, C. Sellitto, B.W. Connors, D.L. Paul, Synchronous activity of inhibitory networks in neocortex requires electrical synapses containing connexin36, Neuron, 31 (2001) 477-485.

D. DeWoskin, J. Myung, M.D. Belle, H.D. Piggins, T. Takumi, D.B. Forger, Distinct roles for GABA across multiple timescales in mammalian circadian timekeeping, Proceedings of the National Academy of Sciences of the United States of America, 112 (2015) E3911-3919.

J.A. Evans, H. Pan, A.C. Liu, D.K. Welsh, Cry1-/- circadian rhythmicity depends on SCN intercellular coupling, Journal of biological rhythms, 27 (2012) 443-452.

E.D. Herzog, J.S. Takahashi, G.D. Block, Clock controls circadian period in isolated suprachiasmatic nucleus neurons, Nature neuroscience, 1 (1998) 708-713.

Z.G. Jiang, Y.Q. Yang, C.N. Allen, Tracer and electrical coupling of rat suprachiasmatic nucleus neurons, Neuroscience, 77 (1997) 1059-1066.

J.R. Jones, D.G. McMahon, The core clock gene Per1 phases molecular and electrical circadian rhythms in SCN neurons, PeerJ, 4 (2016) e2297.

J.R. Jones, M.C. Tackenberg, D.G. McMahon, Manipulating circadian clock neuron firing rate resets molecular circadian rhythms and behavior, Nature neuroscience, 18 (2015) 373-375.

N. Koike, S.H. Yoo, H.C. Huang, V. Kumar, C. Lee, T.K. Kim, J.S. Takahashi, Transcriptional architecture and chromatin landscape of the core circadian clock in mammals, Science, 338 (2012) 349-354.

D. Landgraf, C. Achten, F. Dallmann, H. Oster, Embryonic development and maternal regulation of murine circadian clock function, Chronobiology international, 32 (2015) 416-427.

D. Landgraf, C.E. Koch, H. Oster, Embryonic development of circadian clocks in the mammalian suprachiasmatic nuclei, Frontiers in neuroanatomy, 8 (2014) 143.

A.C. Liu, D.K. Welsh, C.H. Ko, H.G. Tran, E.E. Zhang, A.A. Priest, E.D. Buhr, O. Singer, K. Meeker, I.M. Verma, F.J. Doyle, 3rd, J.S. Takahashi, S.A. Kay, Intercellular coupling confers robustness against mutations in the SCN circadian clock network, Cell, 129 (2007) 605-616.

M.A. Long, M.J. Jutras, B.W. Connors, R.D. Burwell, Electrical synapses coordinate activity in the suprachiasmatic nucleus, Nature neuroscience, 8 (2005) 61-66.

E.S. Maywood, J.E. Chesham, J.A. O'Brien, M.H. Hastings, A diversity of paracrine signals sustains molecular circadian cycling in suprachiasmatic nucleus circuits, Proceedings of the National Academy of Sciences of the United States of America, 108 (2011) 14306-14311.

R.Y. Moore, M.E. Bernstein, Synaptogenesis in the rat suprachiasmatic nucleus demonstrated by electron microscopy and synapsin I immunoreactivity, The Journal of neuroscience : the official journal of the Society for Neuroscience, 9 (1989) 2151-2162.

T. Noguchi, L.L. Wang, D.K. Welsh, Fibroblast PER2 circadian rhythmicity depends on cell density, Journal of biological rhythms, 28 (2013) 183-192.

J. O'Brien, The ever-changing electrical synapse, Current opinion in neurobiology, 29 (2014) 64-72.

H. Ohta, S. Yamazaki, D.G. McMahon, Constant light desynchronizes mammalian clock neurons, Nature neuroscience, 8 (2005) 267-269.

S. Pauls, N.C. Foley, D.K. Foley, J. LeSauter, M.H. Hastings, E.S. Maywood, R. Silver, Differential contributions of intra-cellular and inter-cellular mechanisms to the spatial and temporal architecture of the suprachiasmatic nucleus circadian circuitry in wild-type, cryptochrome-null and vasoactive intestinal peptide receptor 2-null mutant mice, The European journal of neuroscience, 40 (2014) 2528-2540.

J.E. Rash, C.O. Olson, W.A. Pouliot, K.G. Davidson, T. Yasumura, C.S. Furman, S. Royer, N. Kamasawa, J.I. Nagy, F.E. Dudek, Connexin36 vs. connexin32, "miniature" neuronal gap junctions, and limited electrotonic coupling in rodent suprachiasmatic nucleus, Neuroscience, 149 (2007) 350-371.

A.M. Rosenwasser, Circadian drinking rhythms in SHR and WKY rats: effects of increasing light intensity, Physiology & behavior, 53 (1993) 1035-1041.

K. Shinohara, H. Hiruma, T. Funabashi, F. Kimura, GABAergic modulation of gap junction communication in slice cultures of the rat suprachiasmatic nucleus, Neuroscience, 96 (2000) 591-596.

M. Sudo, K. Sasahara, T. Moriya, M. Akiyama, T. Hamada, S. Shibata, Constant light housing attenuates circadian rhythms of mPer2 mRNA and mPER2 protein expression in the suprachiasmatic nucleus of mice, Neuroscience, 121 (2003) 493-499.

M.H. Wang, N. Chen, J.H. Wang, The coupling features of electrical synapses modulate neuronal synchrony in hypothalamic superachiasmatic nucleus, Brain research, 1550 (2014) 9-17.

D.K. Welsh, D.E. Logothetis, M. Meister, S.M. Reppert, Individual neurons dissociated from rat suprachiasmatic nucleus express independently phased circadian firing rhythms, Neuron, 14 (1995) 697-706.

D.K. Welsh, T. Noguchi, Cellular bioluminescence imaging, Cold Spring Harbor protocols, 2012 (2012).

D.K. Welsh, S.M. Reppert, Gap junctions couple astrocytes but not neurons in dissociated cultures of rat suprachiasmatic nucleus, Brain research, 706 (1996) 30-36.

D.K. Welsh, S.H. Yoo, A.C. Liu, J.S. Takahashi, S.A. Kay, Bioluminescence imaging of individual fibroblasts reveals persistent, independently phased circadian rhythms of clock gene expression, Current biology : CB, 14 (2004) 2289-2295.

S.H. Yoo, S. Yamazaki, P.L. Lowrey, K. Shimomura, C.H. Ko, E.D. Buhr, S.M. Siepka, H.K. Hong, W.J. Oh, O.J. Yoo, M. Menaker, J.S. Takahashi, PERIOD2::LUCIFERASE real-time reporting of circadian dynamics reveals persistent circadian oscillations in mouse peripheral tissues, Proceedings of the National Academy of Sciences of the United States of America, 101 (2004) 5339-5346.

A.C. Liu, D.K. Welsh, C.H. Ko, H.G. Tran, E.E. Zhang, A.A. Priest, E.D. Buhr, O. Singer, K. Meeker, I.M. Verma, F.J. Doyle, 3rd, J.S. Takahashi, S.A. Kay, Intercellular coupling confers robustness against mutations in the SCN circadian clock network, Cell, 129 (2007) 605-616.

M.A. Long, M.J. Jutras, B.W. Connors, R.D. Burwell, Electrical synapses coordinate activity in the suprachiasmatic nucleus, Nature neuroscience, 8 (2005) 61-66.

E.S. Maywood, J.E. Chesham, J.A. O'Brien, M.H. Hastings, A diversity of paracrine signals sustains molecular circadian cycling in suprachiasmatic nucleus circuits, Proceedings of the National Academy of Sciences of the United States of America, 108 (2011) 14306-14311.

R.Y. Moore, M.E. Bernstein, Synaptogenesis in the rat suprachiasmatic nucleus demonstrated by electron microscopy and synapsin I immunoreactivity, The Journal of neuroscience : the official journal of the Society for Neuroscience, 9 (1989) 2151-2162.

T. Noguchi, L.L. Wang, D.K. Welsh, Fibroblast PER2 circadian rhythmicity depends on cell density, Journal of biological rhythms, 28 (2013) 183-192.

J. O'Brien, The ever-changing electrical synapse, Current opinion in neurobiology, 29 (2014) 64-72.

H. Ohta, S. Yamazaki, D.G. McMahon, Constant light desynchronizes mammalian clock neurons, Nature neuroscience, 8 (2005) 267-269.

S. Pauls, N.C. Foley, D.K. Foley, J. LeSauter, M.H. Hastings, E.S. Maywood, R. Silver, Differential contributions of intra-cellular and inter-cellular mechanisms to the spatial and temporal architecture of the suprachiasmatic nucleus circadian circuitry in wild-type, cryptochrome-null and vasoactive intestinal peptide receptor 2-null mutant mice, The European journal of neuroscience, 40 (2014) 2528-2540.

J.E. Rash, C.O. Olson, W.A. Pouliot, K.G. Davidson, T. Yasumura, C.S. Furman, S. Royer, N. Kamasawa, J.I. Nagy, F.E. Dudek, Connexin36 vs. connexin32, "miniature" neuronal gap junctions, and limited electrotonic coupling in rodent suprachiasmatic nucleus, Neuroscience, 149 (2007) 350-371.

A.M. Rosenwasser, Circadian drinking rhythms in SHR and WKY rats: effects of increasing light intensity, Physiology & behavior, 53 (1993) 1035-1041.

K. Shinohara, H. Hiruma, T. Funabashi, F. Kimura, GABAergic modulation of gap junction communication in slice cultures of the rat suprachiasmatic nucleus, Neuroscience, 96 (2000) 591-596.

M. Sudo, K. Sasahara, T. Moriya, M. Akiyama, T. Hamada, S. Shibata, Constant light housing attenuates circadian rhythms of mPer2 mRNA and mPER2 protein expression in the suprachiasmatic nucleus of mice, Neuroscience, 121 (2003) 493-499.

M.H. Wang, N. Chen, J.H. Wang, The coupling features of electrical synapses modulate neuronal synchrony in hypothalamic superachiasmatic nucleus, Brain research, 1550 (2014) 9-17.

D.K. Welsh, D.E. Logothetis, M. Meister, S.M. Reppert, Individual neurons dissociated from rat suprachiasmatic nucleus express independently phased circadian firing rhythms, Neuron, 14 (1995) 697-706.

D.K. Welsh, T. Noguchi, Cellular bioluminescence imaging, Cold Spring Harbor protocols, 2012 (2012).

D.K. Welsh, S.M. Reppert, Gap junctions couple astrocytes but not neurons in dissociated cultures of rat suprachiasmatic nucleus, Brain research, 706 (1996) 30-36.

D.K. Welsh, S.H. Yoo, A.C. Liu, J.S. Takahashi, S.A. Kay, Bioluminescence imaging of individual fibroblasts reveals persistent, independently phased circadian rhythms of clock gene expression, Current biology : CB, 14 (2004) 2289-2295.

S.H. Yoo, S. Yamazaki, P.L. Lowrey, K. Shimomura, C.H. Ko, E.D. Buhr, S.M. Siepka, H.K. Hong, W.J. Oh, O.J. Yoo, M. Menaker, J.S. Takahashi, PERIOD2::LUCIFERASE real-time reporting of circadian dynamics reveals persistent circadian oscillations in mouse peripheral tissues, Proceedings of the National Academy of Sciences of the United States of America, 101 (2004) 5339-5346.

Figure 1

Click here to download high resolution image

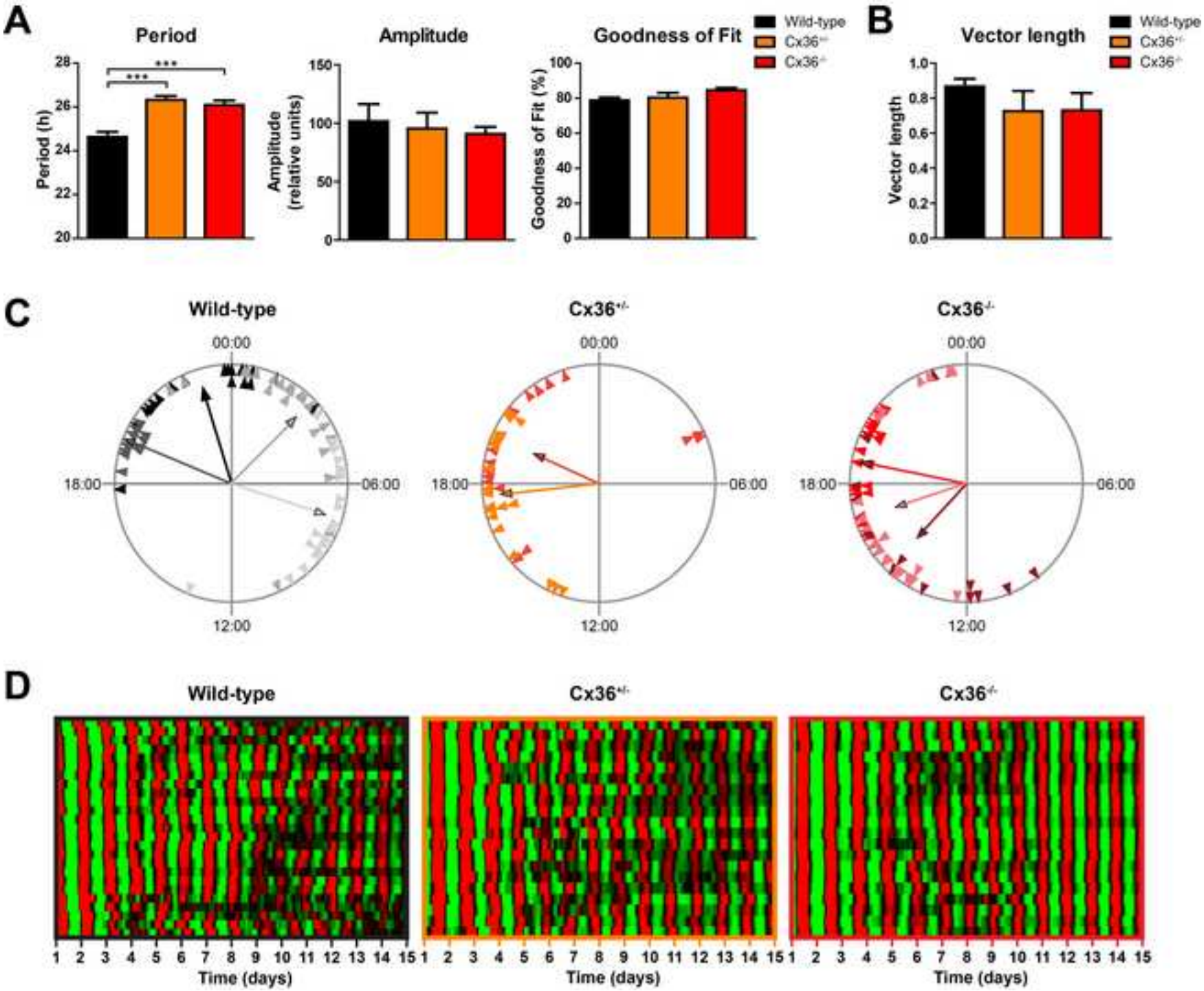

Figure 2

Click here to download high resolution image

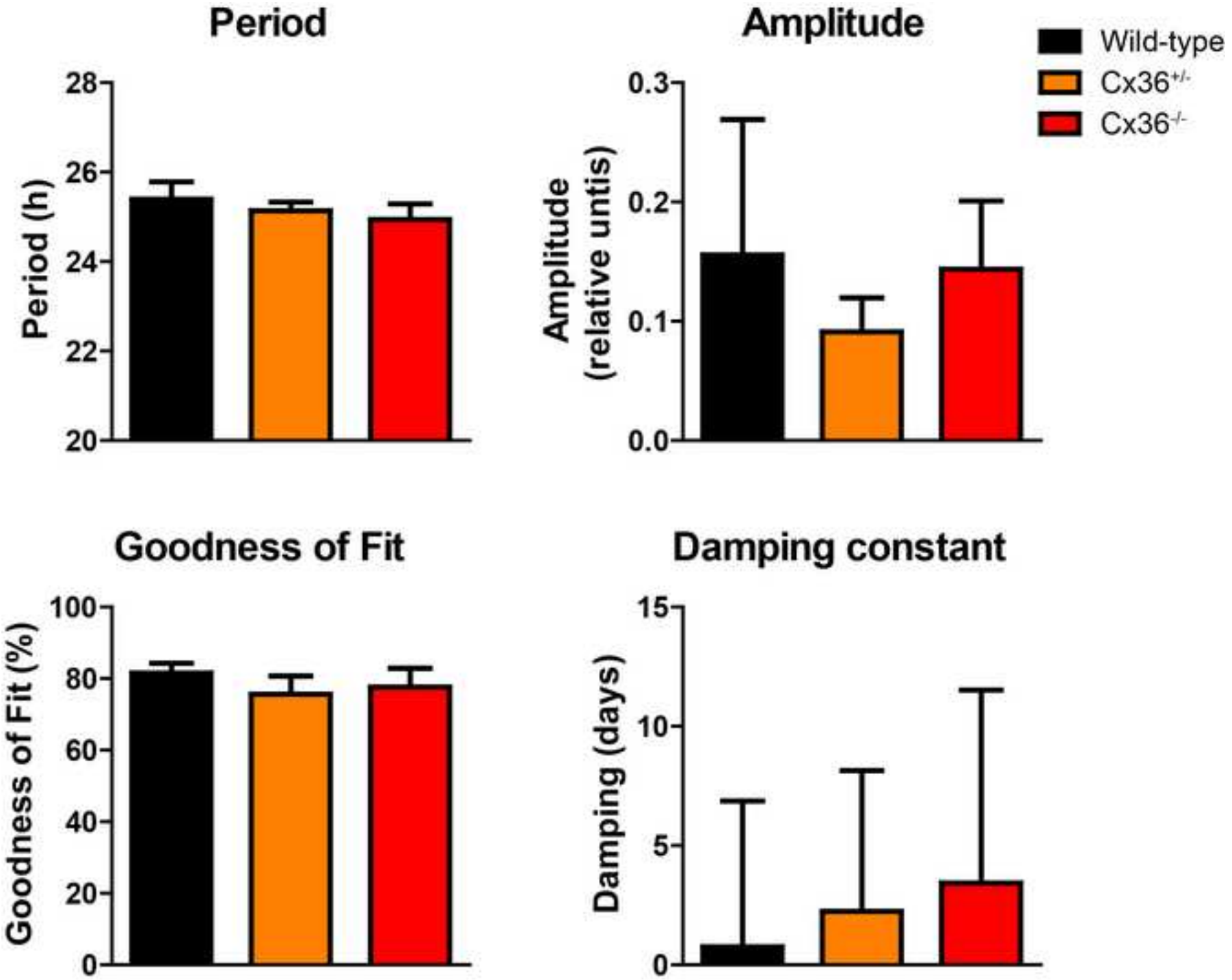

Figure 3

Click here to download high resolution image

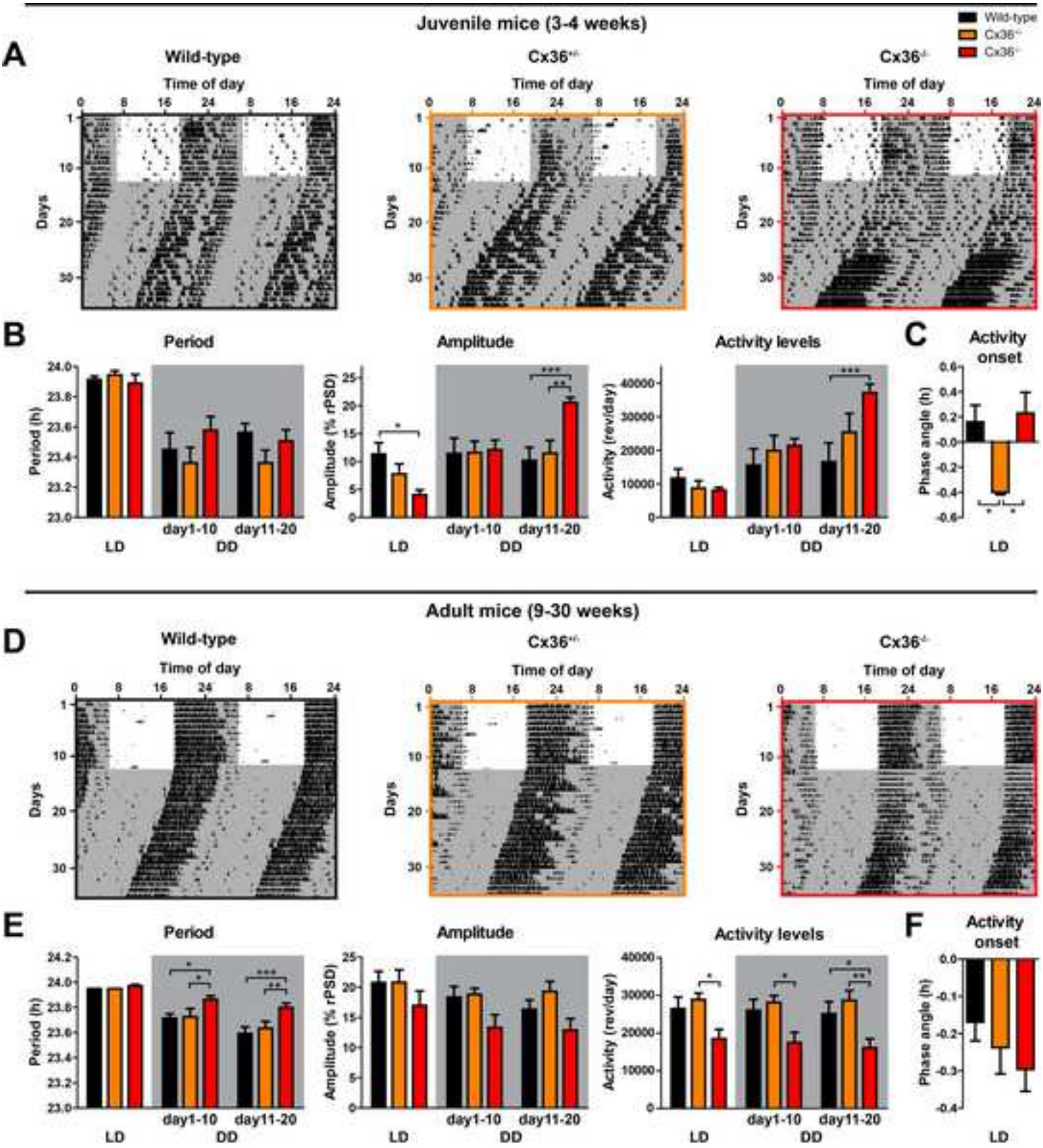

Figure 4

Click here to download high resolution image

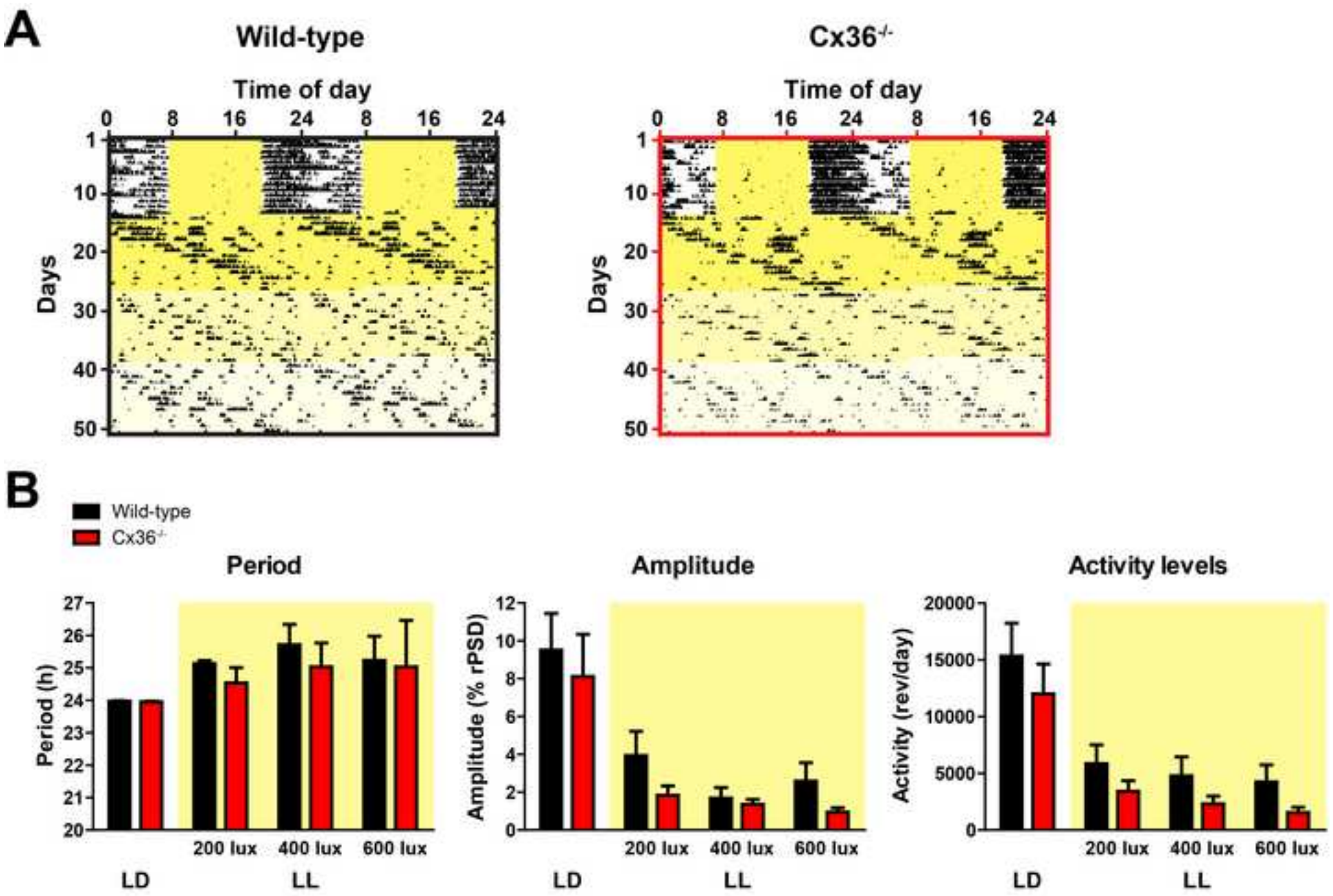

Figure 5

Click here to download high resolution image

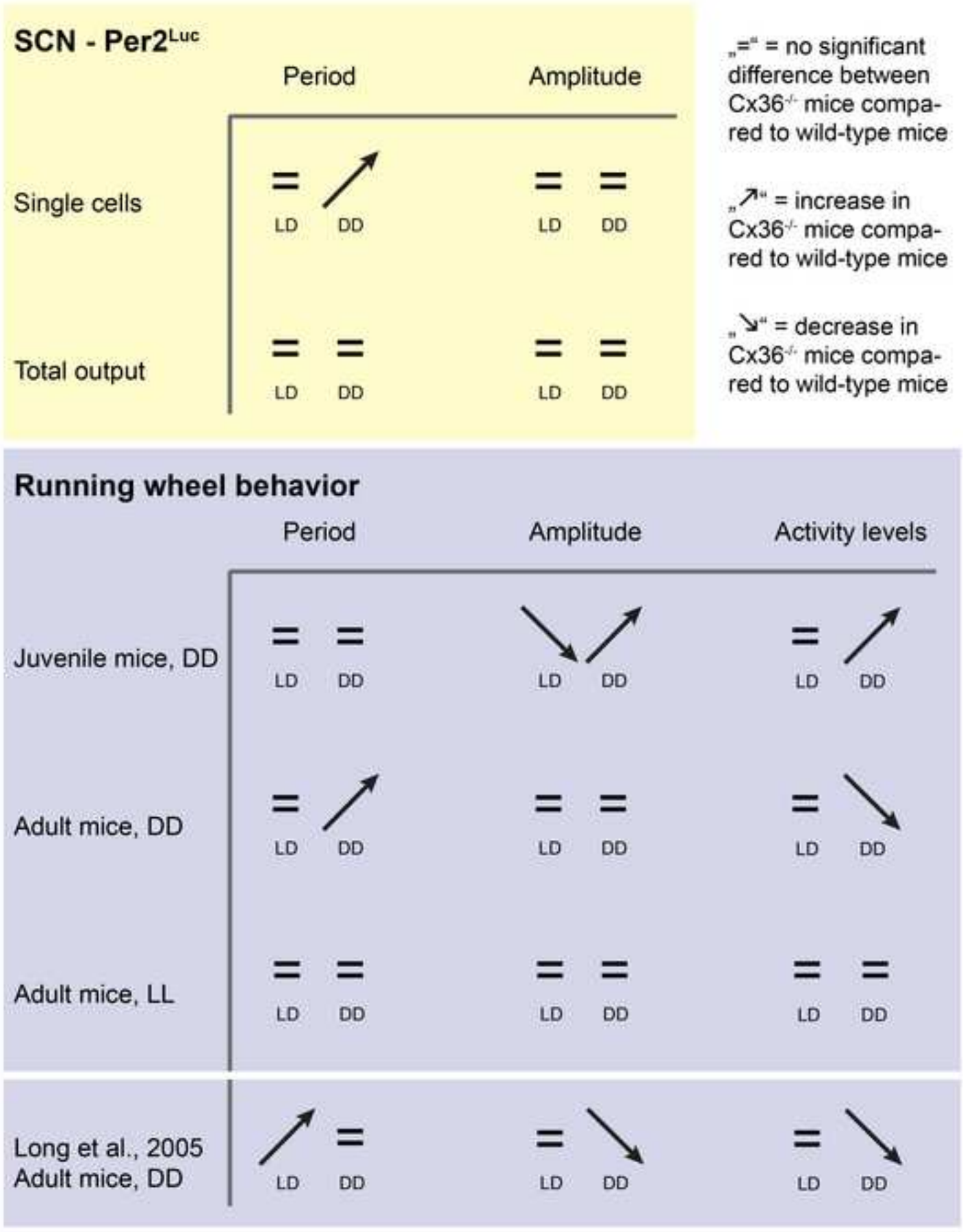

Figure 6

Click here to download high resolution image

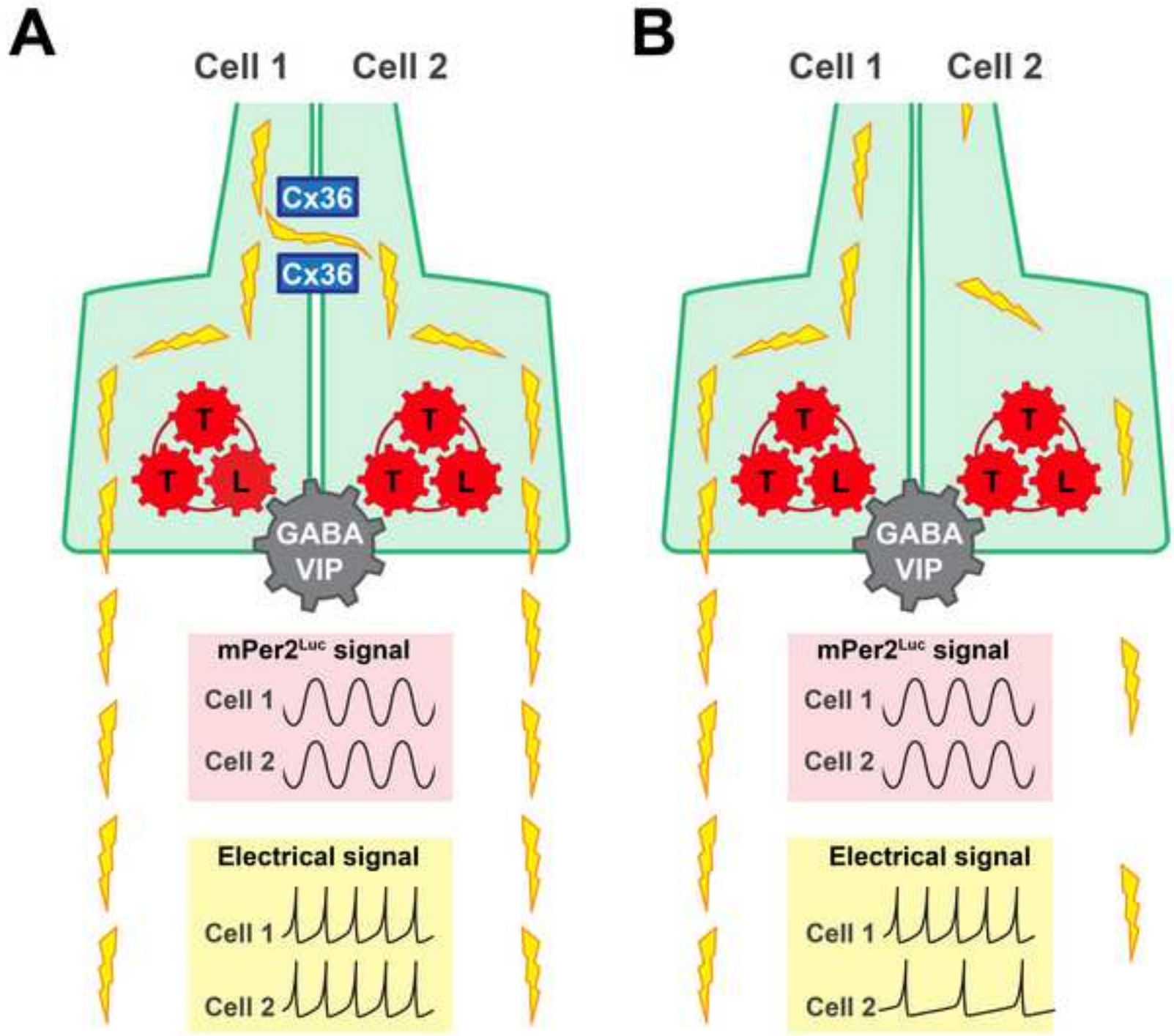

Supplementary Material - Video_WT

Click here to download Supplementary Material - Video(s): SCN_PER2LUC_imag_Cx36-WT_DiemerLandgraf2017.AVI

Supplementary Material - Video_HET

Click here to download Supplementary Material - Video(s): SCN_PER2LUC_imag_Cx36-HET_DiemerLandgraf2017.AVI

Supplementary Material - Video_HOM

Click here to download Supplementary Material - Video(s): SCN_PER2LUC_imag_Cx36-HOM_DiemerLandgraf2017.AVI

Video Still_WT

Click here to download high resolution image

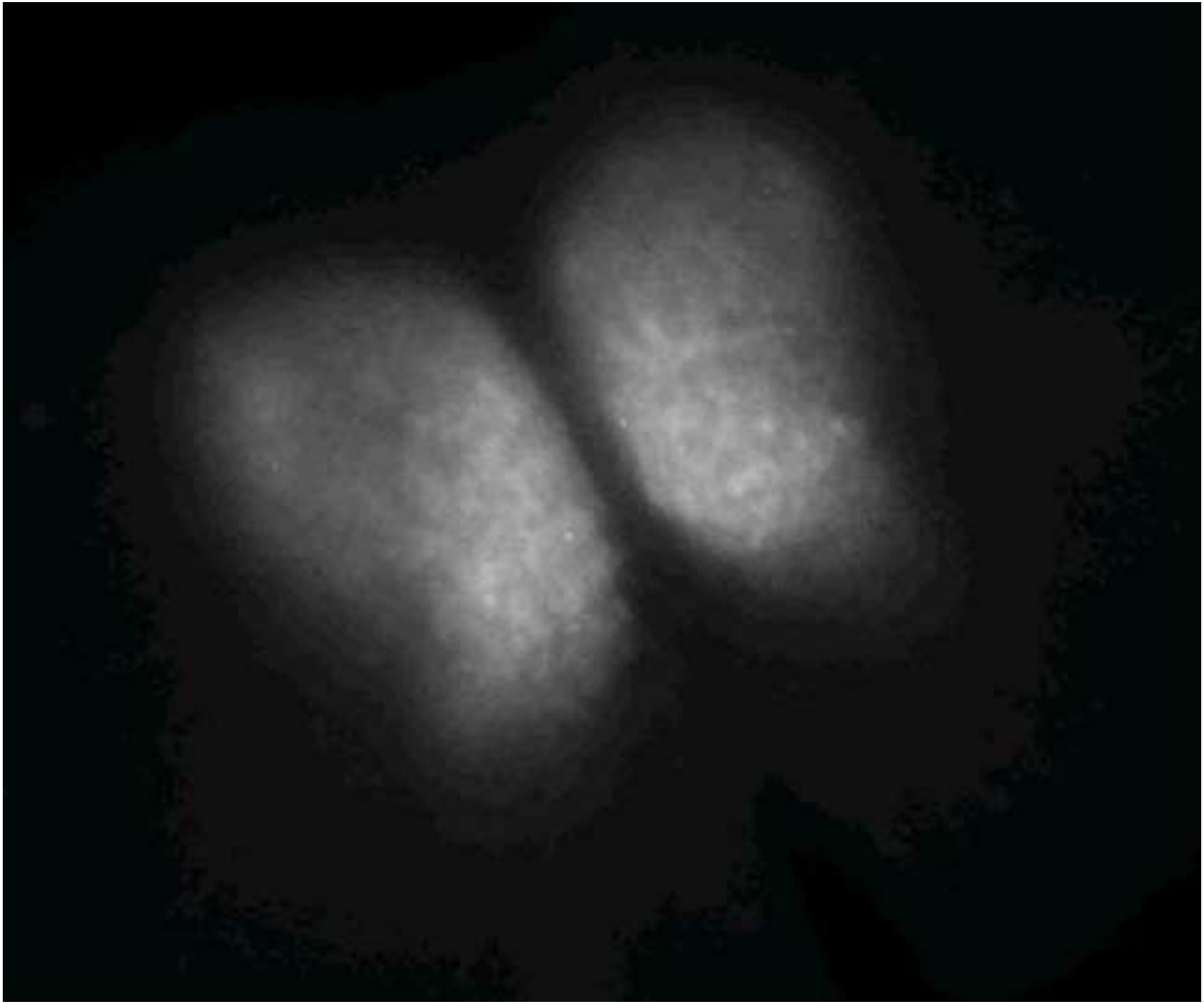

Video Still_HET

Click here to download high resolution image

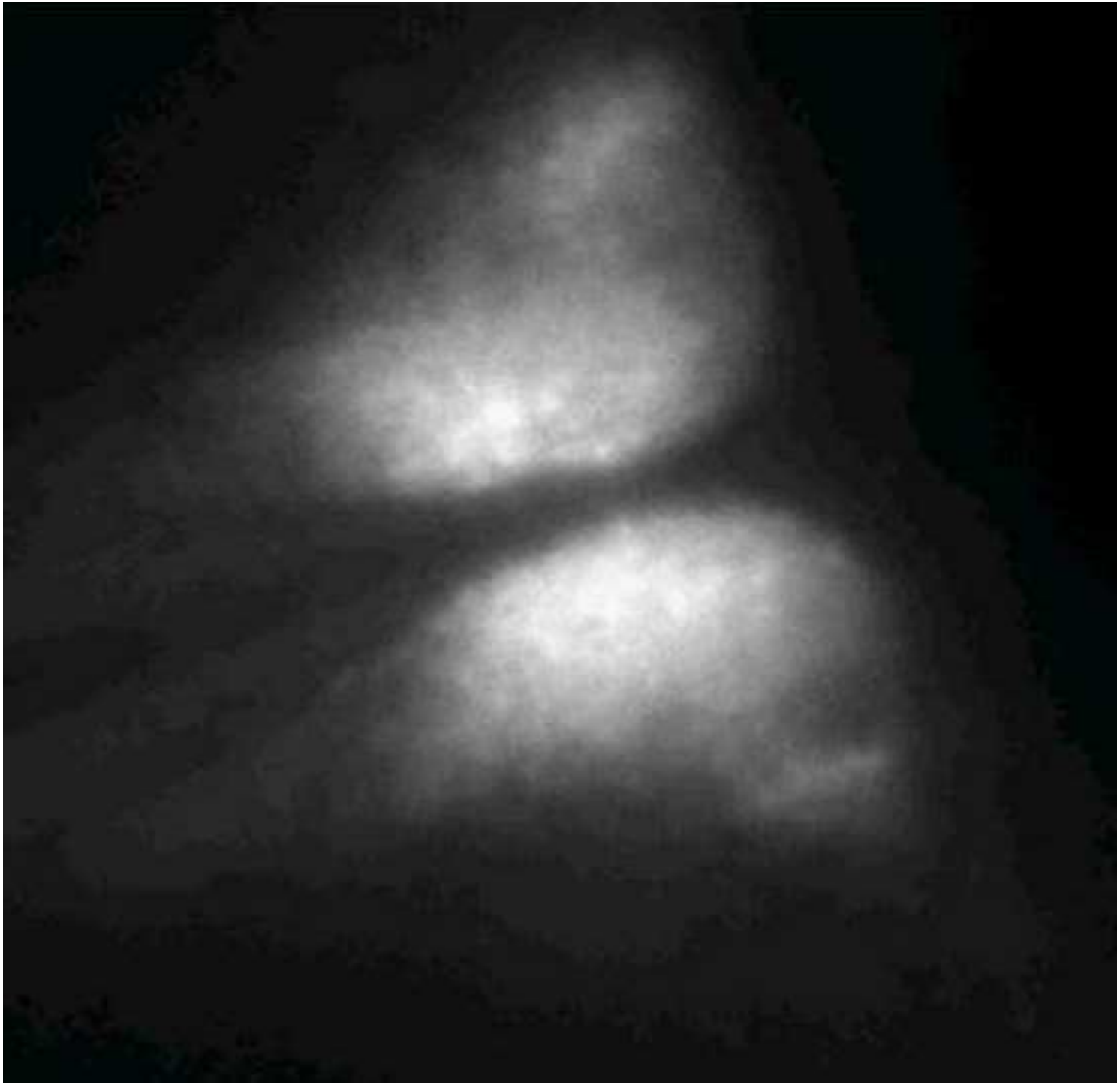

Video Still_HOM

Click here to download high resolution image